THE PUBLISHING HOUSE
OF THE ROMANIAN ACADEMY

PROCEEDINGS OF THE ROMANIAN ACADEMY, Series A,
Volume 14, Number 2/2013, pp. 161–168

COMPARISON OF COMBUSTION CHARACTERISTICS AND HEAT LOSS FOR GASOLINE AND METHANE FUELING OF A SPARK IGNITION ENGINE

Adrian IRIMESCU

"Politehnica" University of Timişoara, Faculty of Mechanical Engineering, Bld. Mihai Viteazul 1, 300222 Timişoara
E-mail: iamotors@yahoo.com

Improved extraction methods have led to increased natural gas production figures, making this fuel a more and more attractive alternative to gasoline. Other advantages such as increased octane rating and reduced carbon dioxide emissions due to lower carbon content also make methane a good candidate for use in spark ignition (SI) engines. An experimental study was performed on a premixed charge SI engine in order to evaluate the differences between gasoline and methane fueling. Based on pressure trace measurements, combustion characteristics and heat losses were analyzed for different engine speed as well as torque settings. Both fuels were found to feature similar combustion duration and cumulative heat loss values. Heat loss distribution during combustion was comparable for the two fuels, with an increase of radiant heat transfer for the gaseous energy source. Methane fueling consistently featured higher indicated fuel conversion efficiency, mainly due to the possibility of spark advance optimization. This resulted in higher pressure levels throughout combustion and improved work output. Also, air–fuel ratios could be shifted closer to stoichiometric compared to gasoline that required slightly richer mixtures to achieve the same level of stability in operation.

Key words: spark ignition engines, gasoline, methane, combustion analysis, heat transfer.

1. INTRODUCTION

In the quest for reducing carbon dioxide emissions and dependency on oil reserves, the study of alternative fuels use in spark ignition (SI) engines is receiving increased attention. Ethanol seems to be the biofuel of choice, given that its production process is well known. Several adaptations are however needed to use this fuel in SI engines, with cold starts being particularly difficult at low ambient temperatures [1]. Methanol can be produced at lower cost and even from atmospheric carbon dioxide and hydrogen [2], but is more toxic than ethanol. Longer chain alcohols such as butanol feature higher heating value, closer to that of gasoline, but their use is hindered by poor evaporative properties [3], a problem also encountered with ethanol. Natural gas is a promising source of energy, given that recent advances in exploration and extraction techniques have made available large reserves [4, 5]. While methane can be used in compression ignition engines as well, application in SI power units is straight forward, and drawbacks such as lower volumetric efficiency and higher NO_x emissions can be relatively easily mitigated [6]. One of the main advantages compared to gasoline is that methane features much higher octane number, thus making possible the optimization of ignition timing [7], while the addition of hydrogen enables stable operation even with lean air-fuel mixtures [8].

Combustion in SI engines is frequently investigated by using in–cylinder pressure analysis. This method uses two parameters, fluid pressure and cylinder volume, that can be determined with good accuracy. By analyzing the pressure trace, several important aspects of engine operation can be evaluated. In this way, valuable information can be obtained on combustion development, as well as the stability and repeatability of this process. This procedure can also be used for evaluating heat transfer from the working fluid to the cylinder walls, relative efficiency compared to constant volume combustion and other performance related parameters [9–11].

Such an analysis was performed in this study using multiple sets of pressure traces recorded for gasoline and methane fueling on a premixed charge SI engine. Multiple engine speed and load settings were investigated for both fuels. Combustion characteristics and cumulative heat loss were calculated based on a first law analysis, using a two zone model. Particular attention was paid to the evaluation of fluid properties, namely the variation of molecular weight variation during combustion. This aspect is generally overlooked when performing pressure trace analysis and was accounted for in order to ensure increased accuracy and a correct evaluation of operational characteristics.

2. EXPERIMENTAL DATA AND PROCEDURE

Pressure measurements performed with an accuracy of ±0.5% on a SI engine with 70 mm bore, 72 mm stroke and 9.6 compression ratio, were evaluated for two different fuel types, namely gasoline and natural gas. Commercial gasoline with a lower heating value (LHV) of 42.9 MJ/kg was used for all liquid fuel trials, while natural gas with a LHV of 46.6 MJ/kg was employed as the gaseous energy source. Several other errors influence pressure measurement such as the choice of a reference point [12] and correct estimation of TDC [13]. Given that air and fuel flow was measured with an accuracy of ±1%, the overall relative error level for indicated fuel conversion efficiency was ±4%. Further details on the experimental procedure are available in [14].

Engine speed and load settings for both fuels, as well as other operational parameters are compiled in Table 1. What is immediately evident is that spark timing – given as crank angle rotation deg before top dead centre (BTDC) – is much more advanced for the gaseous fuel. This in direct connection with the octane number of each fuel, given that spark advance was knock limited. Improved knock resistance also allowed close to stoichiometric operation with methane, given that additional enrichment does not ensure significant increase in combustion stability and laminar flame speed [15]. The consistent improvement in fuel conversion efficiency was also observed with a similar engine [14] and is mainly due to improved spark timing control and a slight shift towards lean operation at each operating point.

Table 1

Operational parameters for all cases investigated

Fuel	Engine speed [rev/min]	Torque [Nm]	Spark timing [deg BTDC]	Relative air–fuel ratio [–]	Indicated efficiency [%]
Gasoline	1500	14	26	0.994	20.2
		47	14	0.993	26.7
		81	6	0.933	26.6
	2000	21	28	0.992	21.4
		49	21	0.993	27.5
		81	12	0.871	25.7
	2500	24	30	0.991	24.5
		52	22	0.992	29.0
		80	10	0.866	27.9
Methane	1500	12	40	0.999	26.2
		36	34	1.003	29.8
		49	28	1.003	31.1
		77	22	0.995	30.1
	2000	10	38	0.999	26.1
		26	36	1.001	30.0
		50	29	0.997	30.5
		77	26	1.001	31.3
	2500	17	38	1.000	29.3
		31	34	0.997	30.4
		56	29	0.989	30.8
		78	24	0.996	31.9

For each combination of engine speed-load settings, a set of 50 consecutive cycles was recorded. The variation of peak pressure values from one cycle to the next can be easily identified in Figs. 1 and 2. No significant difference of this variation can be noticed when comparing the two fuel types. Higher peak pressure values were recorded during methane operation, mainly to the increased spark advance.

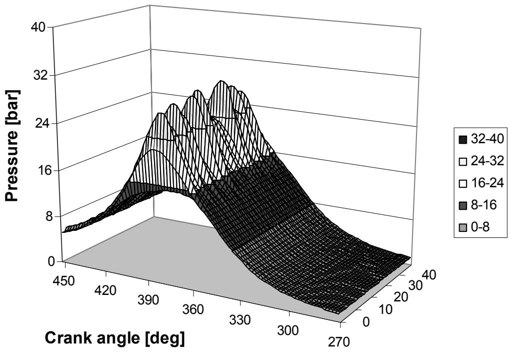

Fig. 1 – Pressure measurement of 50 consecutive cycles for gasoline operation at 2000 rev/min and 49 Nm.

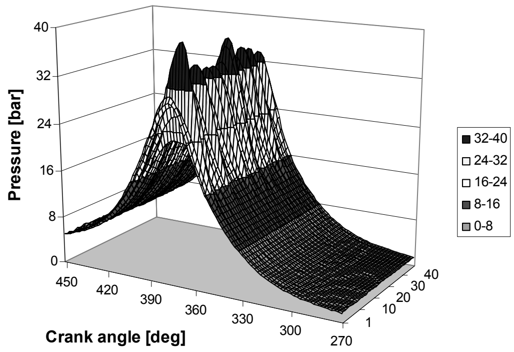

Fig. 2 – Pressure measurement of 50 consecutive cycles for methane operation at 2000 rev/min and 50 Nm.

Both fueling modes used closed loop control, except for full load gasoline operation, when rich air-fuel ratios were employed. At part load all cases investigated featured close to stoichiometric operation (Fig. 3). Higher variation of fuel flow from one cycle to the next for gasoline (Fig. 4) is most likely due to intake port fuel film behavior [16] and pressure pulsations in the fuel line [17].

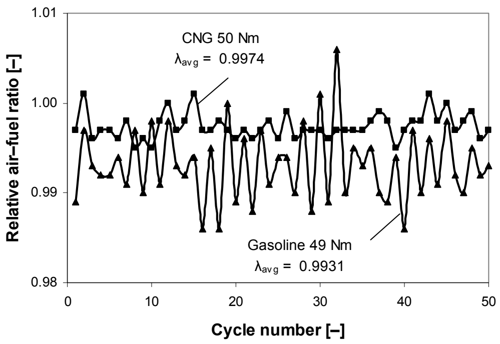

Fig. 3 – Air-fuel ratio variation for 50 consecutive cycles at 2000 rev/min and roughly the same load setting for both fuel types.

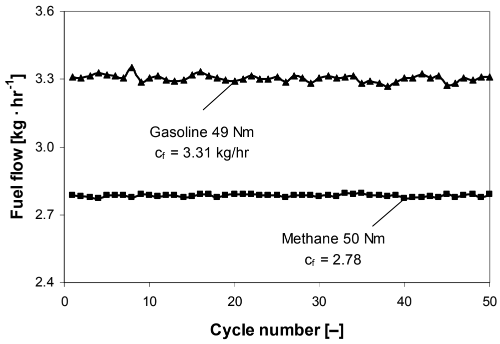

Fig. 4 – Fuel flow variation for 50 consecutive cycles at 2000 rev/min and roughly the same load setting for gasoline and methane fueling.

All sets of pressure traces were analyzed using a two zone (burned and unburned gas) model. Fluid composition can be estimated during combustion by calculating a parameter called mass fraction burned (x_b) [9]. One method used for estimating the mass fraction burned is to calculate a pressure ratio (PR), defined as the ratio of fired and motored pressure traces. This ratio is then used for calculating x_b given by equation (1),

$$x_b = (PR - 1)/(\mathrm{PR}_{\mathrm{EOC}} - 1), \tag{1}$$

where subscript EOC designates the end of combustion. Motored pressure was calculated by considering a constant polytropic coefficient from intake valve closure to start of combustion. Unburned fluid was considered as a mixture of ideal gases (intake charge and residual gas), containing fuel, N_2, O_2, H_2O and CO_2. Therefore, molecular weight values can be calculated for the fresh intake charge and combustion products using equations (2) and (3) respectively,

$$M_{af} = y_{af\,N_2} \cdot M_{N_2} + y_{af\,\mathrm{O}_2} \cdot M_{\mathrm{O}_2} + y_f \cdot M_f, \tag{2}$$

$$M_b = y_{b\,\mathrm{N}_2} \cdot M_{\mathrm{N}_2} + y_{b\,\mathrm{O}_2} \cdot M_{\mathrm{O}_2} + y_{b\,\mathrm{H_2O}} \cdot M_{\mathrm{H_2O}} + y_{b\,\mathrm{CO}_2} \cdot M_{\mathrm{CO}_2}, \tag{3}$$

where M is the molecular weight measured in kg/kmol, with subscript *af* for air-fuel mixture, *b* for burned gas and *f* for fuel, *y* is the mole fraction, with the same meaning of subscripts as for *M*.

Overall molecular weight for the working fluid during compression was calculated using equation (4),

$$M_u = 1/\left(x_{af}/M_{af} + x_r/M_b\right), \tag{4}$$

where subscript u denotes unburned mixture. During combustion formula (5) was employed,

$$M = 1/\left(\left(1 - x_b\right)/M_u + x_b/M_b\right), \tag{5}$$

and using the equation of state for ideal gases, fluid temperature (T) could be calculated throughout the closed valves part of the cycle,

$$T = \frac{p \cdot V \cdot M}{m \cdot R}, \tag{6}$$

where p is the fluid pressure measured in Pa, V the cylinder volume in m^3, m is the cylinder charge mass measured in kg, considered as constant from intake valve closure to exhaust valve opening, and R the universal constant for ideal gases in J / (kmol · K).

Constant pressure specific heat (c_p) for each component was calculated using hyperbolic functions [18],

$$c_p = \frac{1}{M} \cdot \left(C_1 + C_2 \cdot \left(\frac{C_3/T}{\sinh\left(C_3/T\right)} \right)^2 + C_4 \cdot \left(\frac{C_5/T}{\cosh\left(C_5/T\right)} \right)^2 \right), \tag{7}$$

that were found to ensure an accuracy of 1% or better up to 3 000K, when compared to values predicted by more complex polynomial functions [19]. Temperature values in equation (7) are taken as different for burned and unburned gas in order to ensure increased accuracy, and are measured in K, same as constants C_3 and C_5, while C_1, C_2 and C_4 are measured in J / (kmol K). Constant volume specific heat was calculated using the ideal gas assumption, $c_v = c_p - R / M$.

Based on the energy balance, combined with the equation of state for ideal gases, a so called 'net heat release rate' (dQ) can be calculated. After substitution and rearrangement, equation (8) can be written,

$$\mathrm{d}Q = \frac{\gamma}{\gamma - 1} \cdot p \cdot \mathrm{d}V + \frac{1}{\gamma - 1} \cdot V \cdot \mathrm{d}p + \frac{1}{\gamma - 1} \cdot p \cdot V \cdot \frac{\mathrm{d}M}{M}, \tag{8}$$

where Q is measured in J and γ is the ratio of specific heats. It should be noted that all variable parameters are integrated with respect to crank angle rotation. For illustrative purposes, this aspect will not be mentioned.

The term dQ in equation (8) can be expressed as $\mathrm{d}Q = \mathrm{d}Q_f - \mathrm{d}Q_{in} - \mathrm{d}Q_{ht}$, with $\mathrm{d}Q_f = \mathrm{d}x_b \cdot m_f \cdot$ LHV as the heat released through fuel oxidation, $\mathrm{d}Q_{in}$ heat lost due to incomplete combustion and dissociation, while $\mathrm{d}Q_{ht}$ refers to the heat transferred to the combustion chamber walls. Most studies combine $\mathrm{d}Q_f - \mathrm{d}Q_{in}$ and relate to this term as the real heat of combustion. Given the scope of this analysis, losses due to incomplete combustion were taken as $\mathrm{d}Q_{in} = (1 - \lambda)\, \mathrm{d}Q_f$ for slightly rich mixtures and were ignored for stoichiometric and slightly lean operation. This is somewhat questionable, given that it artificially increases calculated heat losses. However, given that combustion inefficiency should be roughly the same for both fuels no major influence on the comparison between gasoline and methane fueling is likely.

3. RESULTS AND DISCUSSION

Cumulative heat loss calculated based on a first law analysis was investigated for both fuels at roughly the same load and three different engine speed settings in order to investigate the effect of this operational parameter (Fig. 5). Given that determining combustion efficiency was beyond the scope of this work, heat loss listed throughout the article is referenced to the heating value of the fuel contained within the combustion chamber (Q_f), without identifying the nature of the loss (i.e. that is heat transfer, incomplete fuel oxidation or combustion product dissociation). Methane and gasoline operation featured the same slightly decreasing trend in heat loss variation as engine speed increased. The slight difference in the shape of each curve can be attributed to statistical distribution of measurements rather than a fuel effect. In order to evaluate the effect of load variation on heat losses, four torque settings were evaluated at three different engine speed values with methane fueling (Fig. 6). Only a slight increase of heat loss was observed for 1 500 and 2 000 rev/min as load increased, while for operation at 2 500 rev/min hardly any variation was observed, in line with other measurements performed with this fuel [20].

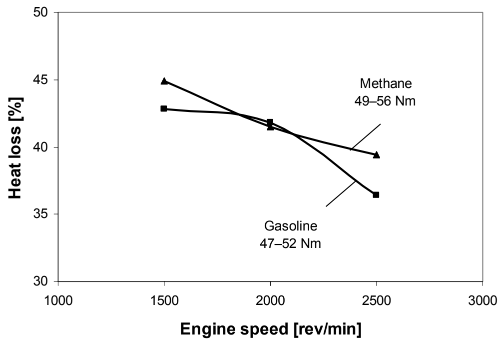

Fig. 5 – Cumulative heat loss at different engine speed settings.

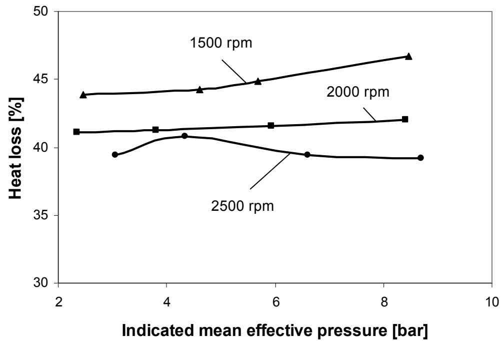

Fig. 6 – Cumulative heat loss for methane fueling at different load settings.

Given that no significant differences in heat loss variation with the increase of engine speed and load were noticed for the two fuel types, two sets of pressure traces recorded at 2 000 rev/min and very close torque settings (49 Nm with gasoline and 50 Nm for methane) were evaluated in detail.

Higher peak pressure values were recorded for methane operation (Fig. 7), mainly due to the advanced ignition timing. Temperature traces follow a similar trend towards the end of compression and beginning of expansion strokes (Fig. 8), and featured higher values for the liquid fuel at the end of combustion and after its completion. This is in connection with slightly increased pressure towards the end of expansion for gasoline and lower overall fluid molecular weight when using the gaseous fuel (27.6 kg/kmol for the case of methane as compared to 30.2 for unburned and 28.8 kg/kmol for burned gas with gasoline, at similar residual gas fractions).

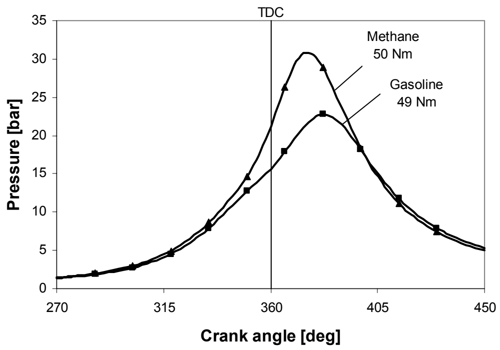

Fig. 7 – Pressure traces for gasoline and methane at 2000 rev/min.

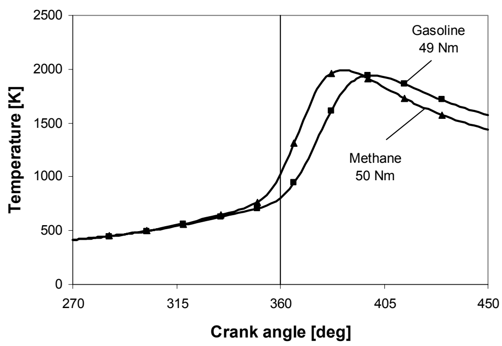

Fig. 8 – Temperature traces for gasoline and methane at 2000 rev/min.

Given that both fuel types feature comparable laminar flame speed values, combustion duration and heat release rate shape are similar when gasoline or methane was used (Fig. 9). A slightly higher peak was recorded for the rate of heat release with the gaseous fuel, as spark timing was advanced compared to gasoline operation. Mass fraction burned (MFB) profiles were also similar for the two fuel types (Fig. 10). An interesting observation is that while the first (from 0 to 1% MFB) and main (from 1 to 90% MFB) phases of combustion featured comparable duration and heat loss, a prolonged final stage was noticed for methane and higher heat loss as a result (Table 2). This effect was consistent for all cases investigated and requires further study for a clear explanation.

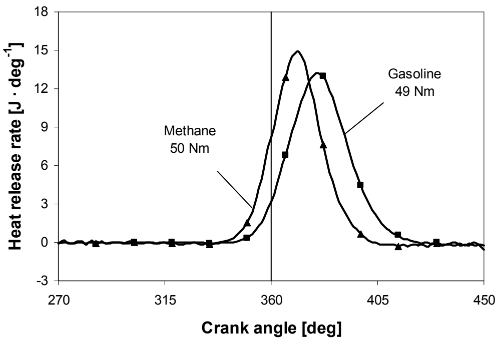

Fig. 9 – Rate of heat release for gasoline and methane operation at 2000 rev/min.

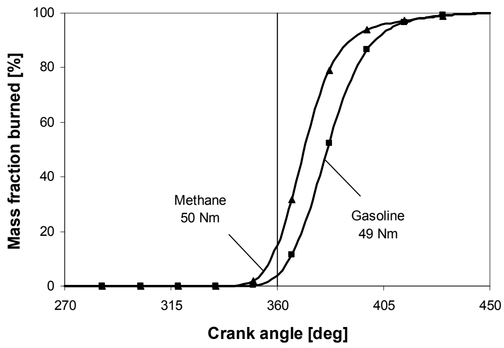

Fig. 10 – Mass fraction burned for gasoline and methane operation at 2000 rev/min.

Table 2

Combustion related parameters for 2000 rev/min and ~50 Nm torque

Fuel	Combustion duration [deg]			Heat loss* [%]		
Mass fraction burned	0–1%	1–90%	90–100%	0–1%	1–90%	90–100%
Gasoline	18	46	46	0.3	25.1	7.1
Methane	18	44	58	0.4	23.0	9.5

* referenced to the heating value of the fuel inside the combustion chamber

Heat transfer through radiation is generally considered as insignificant for gasoline engines and only convection is evaluated. In order to investigate if the different air–fuel mixture and burned gas composition has a significant influence when using methane instead of gasoline, emissivity (Fig. 11) and thermal conductivity (Fig. 12) values were calculated for both fuel types under similar engine speed and load settings.

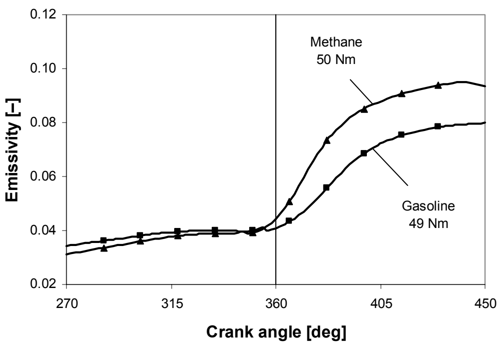

Fig. 11 – Calculated bulk gas emissivity for gasoline and methane fueling at 2000 rev/min.

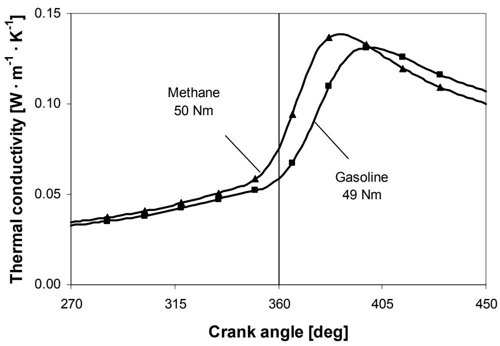

Fig. 12 – Calculated bulk gas thermal conductivity for gasoline and methane fueling at 2000 rev/min.

Higher burned gas emissivity was obtained for methane fueling (Fig. 11), mainly because of icreased partial pressure of CO_2 and H_2O (peak $p_{CO_2} + p_{H_2O} = 8.79$ bar as compared to 5.95 bar for gasoline burned gas), as well as different burned gas composition ($y_{CO_2} + y_{H_2O} = 28.5\%$ as compared to 26.2% bar for the classical fuel). This is of some importance for biogas fueling, given that CO_2 volumetric concentrations can be as high as 50% for this fuel type, thus significantly increasing radiant heat losses. However, given that this heat transfer mechanism is far less important compared to convection, the advantage of high octane rating combined with increased spark advance should ensure similar gain in fuel conversion efficiency when using biogas compared to gasoline operation. The curves for thermal conductivity closely follow the trend of the temperature traces (Fig. 12), with close values for both fuel types.

In order to give a more accurate idea of how each transfer mechanism influences losses throughout the working cycle, cumulative heat loss values were compiled in Table 3. This analysis reveals that radiation is insignificant during compression, mainly because of low gas temperature, as well as reduced gas emissivity. Heat losses between intake valve closure and ignition when using the gaseous fuel were consistently higher for all cases investigated. Convective heat transfer during combustion was comparable for both fuel types, while radiation was increased by up to 20% when using methane instead of gasoline. Again, this may be of greater importance for biogas fueling, given that this operational strategy results in high concentrations of CO_2 in the working fluid. However, when comparing convection to heat losses due to radiation, it is obvious that this effect should have somewhat reduced significance.

Table 3

Heat loss distribution throughout the working cycle at 2000 rev/min and ~50 Nm torque

Fuel	Heat loss* [%]								
	Compression			Combustion			Expansion		
	Convection	Radiation	Total	Convection	Radiation	Total	Convection	Radiation	Total
Gasoline	0.4	<0.1	0.4	31.7	0.8	32.5	8.5	0.3	8.8
Methane	0.9	<0.1	0.9	31.9	1.0	32.9	7.3	0.3	7.6

4. CONCLUSION

Several sets of in-cylinder pressure traces recorded for gasoline and methane fueling at different engine speed and load settings were investigated in order to analyze combustion characteristics and heat losses for the two fuel types. One major conclusion of this study was that methane operation ensured an increase of up to 30% (relative difference) in indicated fuel conversion efficiency compared to gasoline, especially at low load settings.

Cumulative heat loss was found to be at similar levels for both fuels, within the 35–45% range at roughly the same torque level and three different rotational speed values of 1 500, 2 000 and 2 500 rev/min. A decrease of heat losses was recorded at engine speed increased, while load variation was found to have only a minor influence on this parameter.

A more detailed analysis of 50 consecutive cycles each, at 2 000 rev/min and 49–50 Nm torque, revealed that methane fueling featured higher peak pressure values and roughly the same temperature levels. The main reason for this was the possibility to increase ignition advance due to the high octane number of the gaseous fuel. Net heat release rates and mass fraction burned profiles were similar, with major differences also due to increased spark advance for methane. Lower heat losses due radiation of up to 20% for gasoline were found to be due to higher gas emissivity for methane fueling. Thermal conductivity was at similar levels for both fuel types, thus resulting in comparable cumulative heat loss values due to convection.

ACKNOWLEDGEMENTS

This work was partially supported by the strategic grant POSDRU/89/1.5/S/57649, Project ID 57649 (PERFORM-ERA), co-financed by the European Social Fund – Investing in People, within the Sectoral Operational Programme Human Resources Development 2007–2013. The contribution of Emiliano Pipitone from the University of Palermo is also gratefully acknowledged.

REFERENCES

1. SALES L. C. M., SODRE J. R., *Cold start characteristics of an ethanol-fuelled engine with heated intake air and fuel*, Applied Thermal Engineering, **40**, pp. 198–201, 2012.
2. VANCOILLIE J., DEMUYNCK J., SILEGHEM L., VAN DE GINSTE M., VERHELST S., *Comparison of the renewable transportation fuels, hydrogen and methanol formed from hydrogen, with gasoline – Engine efficiency study*, International Journal of Hydrogen Energy, **37**, *12*, pp. 9914–9924, 2012.
3. IRIMESCU A., *Performance and fuel conversion efficiency of a spark ignition engine fueled with iso-butanol*, Applied Energy, **96**, pp. 477–483, 2012.
4. COHEN G., JOUTZ F., LOUNGANI P., *Measuring energy security: Trends in the diversification of oil and natural gas supplies*, Energy Policy, **39**, *9*, pp. 4860–4869, 2011.
5. ASCHE F., OGLEND A., OSMUNDSEN P., *Gas versus oil prices the impact of shale gas*, Energy Policy, **47**, pp. 117–124, 2012.

6. KORAKIANITIS T., NAMASIVAYAM A. M., CROOKES R. J., *Natural-gas fueled spark-ignition (SI) and compression-ignition (CI) engine performance and emissions*, Progress in Energy and Combustion Science, **37**, *1*, pp. 89–112, 2011.
7. BRADLEY D., *Combustion and the design of future engine fuels*, Proceedings of the Institution of Mechanical Engineers, Part C: Journal of Mechanical Engineering Science, **223**, *12*, pp. 2751–2765, 2009.
8. MORENO F., MUNOZ M., ARROYO J., MAGÉN O., MONNÉ C., SUELVES I., *Efficiency and emissions in a vehicle spark ignition engine fueled with hydrogen and methane blends*, International Journal of Hydrogen Energy, in Press, Corrected Proof; doi:10.1016/j.ijhydene.2012.04.012, 2012.
9. HEYWOOD J. B., *Internal Combustion Engine Fundamentals*, Mc-Graw Hill Series in Mechanical Engineering, 1988.
10. SHUDO T., NABETANI S., NAKAJIMA Y., *Analysis of the degree of constant volume and cooling loss in a spark ignition engine fuelled with hydrogen*, International Journal of Engine Research, **2**, *1*, pp. 81–92, 2001.
11. SHEHATA M. S., *Cylinder pressure, performance parameters, heat release, specific heats ratio and duration of combustion for spark ignition engine*, Energy, **35**, *12*, pp. 4710–4725, 2010.
12. MAURYA R. K., AGARWAL A. K., *Investigations on the effect of measurement errors on estimated combustion and performance parameters in HCCI combustion engine*, Measurement, in Press, Accepted Manuscript; doi:10.1016/j.measurement.2012.05.021, 2012.
13. PIPITONE E., BECCARI A., *Determination of TDC in internal combustion engines by a newly developed thermodynamic approach*, Applied Thermal Engineering, **30**, *14–15*, pp. 1914–1926, 2010.
14. PIPITONE E., BECCARI S., *Performances improvement of a S.I. CNG bi-fuel engine by means of double-fuel injection*, 9th International Conference on Engines and Vehicles, Naples, Italy, Session: SI Combustion Experiments, SAE Paper No 2009-24-0058, 2009.
15. D'ERRICO G., *Prediction of the combustion process and emission formation of a bi-fuel s.i. engine*, Energy Conversion and Management, **49**, *11*, pp. 3116–3128, 2008.
16. IIDA M., YOSHIKAWA K., TANAKA H., WANG G., ARCOUMANIS C., *Fuel Film Behavior Analysis Using Simulated Intake Port*, SAE Paper No 2009-32-0129, 2009.
17. HEO H. S., BAE S. J., LEE H. K., PARK K. S., *Analytical study of pressure pulsation characteristics according to the geometries of the fuel rail of an MPI engine*, International Journal of Automotive Technology, **13**, *2*, pp. 167–173, 2012.
18. GREEN D. W., PERRY R. H., *Perry's Chemical Engineers' Handbook, Eighth Edition*, McGraw-Hill, New York, 2007.
19. *** NIST Chemistry WebBook, http://webbook.nist.gov, April 2012.
20. SIERENS R., DEMUYNCK J., DE PAEPE M., VERHELST S., *Heat Transfer Comparison between Methane and Hydrogen in a Spark Ignited Engine*, 18th World Hydrogen Energy Conference, Essen, Germany, May 16–21, pp. 148–156, 2010.

Received June 26, 2013